Structural and photoluminescence properties of Ge–Si ultra-thin films and heterostructures

2002 J. Phys.: Condens. Matter 14 8333

(http://iopscience.iop.org/0953-8984/14/35/307)

INSTITUTE OF PHYSICS PUBLISHING JOURNAL OF PHYSICS: CONDENSED MATTER

J. Phys.: Condens. Matter **14** (2002) 8333–8351 PII: S0953-8984(02)33991-2

Structural and photoluminescence properties of Ge–Si ultra-thin films and heterostructures

P Castrucci[1], **R Gunnella**[1,2], **N Pinto**[1] **and M De Crescenzi**[1,3]

[1] Dipartimento di Fisica, Unita' INFM, Universita' di Camerino Via Madonna delle Carceri, 62032 Camerino, Italy
[2] INFN-LNF, PO Box 13, Frascati, Italy

Received 19 February 2002, in final form 29 April 2002
Published 22 August 2002
Online at stacks.iop.org/JPhysCM/14/8333

Abstract

This paper reviews recent advances in our current level of understanding of the physics underlying the growth process of Ge thin films, $(Ge_nSi_n)_p$ superlattices and GeSi heterostructures on the Si(001)2 × 1 reconstructed surface. The role of thermodynamics and silicon surface reconstruction is discussed, together with the effects of Sb as a surfactant. Careful investigation of structural and photoluminescence properties is reported.

1. Introduction

A great impulse to the scientific community's interest in GeSi-based materials has been given by the experimental observation of optical transitions in thin $(Ge_mSi_n)_p$ short-period, strained-layer superlattices grown on Si(001) (Pearsall *et al* 1989). These measurements, in fact, made GeSi-based systems interesting both for their fundamental physical properties and for the possibility to develop GeSi-based optoelectronic devices integrated on silicon-based technology. Then, several theoretical studies appeared to explain these experimental observations and predicted similar phenomena for other suitably grown samples. The basic idea was that superlattices grown by depositing a few (m, n) combinations of atomically controlled layers produced direct- or quasi-direct bandgaps (Schmid *et al* 1991, Zachai *et al* 1990, Tserbak *et al* 1993) as a combined result of strain and zone-folding effects. These results would imply that, starting from indirect-gap semiconductors such as pure Ge and pure Si and acting on the number of atomic layers constituting the heterostructure, photoemitters with different values of the direct or quasi-direct optical transition energy could be obtained. The interest generated by these theoretical predictions led to many experimental efforts (Presting *et al* 1992) addressed to the identification of growth conditions able to provide such desired materials. For the last decade researchers have been following two main and closely connected directions: the former has looked for Ge–Si systems able to be good candidates for technology; the latter has employed large resources to deeply understand the first stages of Ge growth on differently

[3] Permanent address: Dipartimento di Fisica, Unita' INFM, Universita' di Roma Tor Vergata, 00133 Roma, Italy.

oriented silicon substrates. Ge–Si systems are, in fact, characterized by a considerable lattice mismatch, because the Ge crystal lattice is about 4% larger than that of Si. It is generally accepted that initial stages of growth for systems with such a large lattice misfit take place in a layer-by-layer fashion, i.e. the grown layers are in registry with the substrate layers; the lattice constant in the perpendicular direction expands, leading to a tetragonal distortion. However, as the film thickness increases, the strain energy accumulates and the system needs to lower its free energy. The highest thickness which an overlayer can sustain is generally called the critical thickness. Different mechanisms can be claimed to occur when exceeding the critical coverage: generation of misfit dislocations, growth of coherent islands, introduction of missing atoms rows and intermixing; the first three growth mechanisms mainly relieve the strain energy, the last one principally reduces the total energy of the film. Very many theoretical and experimental results, mainly dealing with the study of these processes, have been published. A general accordance has been difficult to obtain. In particular, for a long time intermixing between Ge and Si at silicon surfaces has been considered unlikely, while strain relief mechanisms are still incompletely and unsatisfactorily explained. In any case, since the early 1990s two points have been universally accepted: Ge overlayer growth occurs differently because of (i) differently oriented silicon substrates and (ii) sample growth and/or annealing temperature. Very soon the Si(001) surface turned out to be the technologically promising one and the Si(111) and the other silicon substrate orientations have been less studied. On the other hand, the use of surfactants, in particular As and Sb, which segregate to the surface, has been introduced and extensively studied to prevent island formation and intermixing (Copel *et al* 1989, Copel and Tromp 1991, LeGoues *et al* 1989) and to improve the photoluminescence (PL) properties of the heterostructures (Noel *et al* 1989, 1990). In this scenario the importance of using experimental techniques with a great sensitivity to the structural environment in terms of element types and lattice parameters and at the same time performing PL experiments is clear. X-ray absorption spectroscopy (XAS) and core-level electron diffraction are techniques able to retrieve non-destructive information relating to the growth morphology and structural environment of thin epitaxial layers. X-ray absorption is an element-selective probe of the partial unfilled density of states (DOS) and thus is a suitable technique to monitor any change in the electronic structure above E_F (Fermi level). Therefore, hidden in each near-edge spectral lineshape is information on the local structure around the emitter atom (Stöhr 1992). In particular, any effects induced by small changes in the atomic structure will affect preferentially those empty energy bands which exhibit a high degree of localization around the specified atom. An XPD (x-ray photoelectron diffraction) pattern and its Auger counterpart (Auger electron diffraction, AED) report the modulations of the measured current, usually from a core level, as a function of the kinetic energy and/or the emission direction of the analysed photoelectrons. These modulations are due to the interference between the primary photoelectronic wave and the portions of this wave elastically scattered by the atoms surrounding the photoabsorber. Their study, therefore, provides local structural information around the emitter atom (Egelhoff 1990, Fadley 1990). At high photoelectron energies ($E_{kin} \geqslant 500$ eV) these patterns can be easily interpreted in terms of forward scattering along directions connecting neighbour atoms to the emitter (Fadley 1990). Since 1995, we have independently used such tools to study the case of Ge and $(Ge_mSi_n)_p$ growth on Si(001) to obtain information on strain, roughness and intermixing as a function of growth parameters and/or surfactant presence. In particular, we obtained unambiguous proof of Ge–Si atom site exchange at the Ge/Si(001) interface in the case of a few monolayers of Ge deposited at both RT and 400 °C or annealed (Gunnella *et al* 1996, Castrucci *et al* 1998a, 1998b). Moreover, we determined the strain content of the overlayers and showed that films grown at RT are characterized by a higher amount of strain than ones grown at 400 °C or post-growth annealed (Gunnella *et al* 1996, Castrucci *et al*

1998a). We succeeded in selecting the intermixed structural model, among those proposed in the literature, best fitting the XAS experimental data. In fact, different atomic elements are found to preferentially arrange according to a double-layer ordering mechanism along the ⟨111⟩ crystallographic directions (Castrucci *et al* 1998a). A similar evaluation has been carried out for $(Ge_2Si_2)_{15}$ multilayers grown on Si(001) surface (Castrucci *et al* 1998c). We also investigated the effects of Sb as a surfactant on the Si(001) interface by using electron diffraction tools. In this case, indications of a laminar growth of the strained Ge overlayer, with reduced intermixing, are obtained when 1 ML of Sb is predeposited on the substrate and the deposition is carried out keeping the substrate at temperatures lower than or equal to 400 °C. When annealing and/or deposition at higher temperature are performed, hints of a sizeable intermixing and/or roughness of the film have been detected. An evaluation of 3 and 6 ML film strain content is obtained (Gunnella *et al* 1998). Finally we found the effectiveness of Sb action in a $(Ge_4Si_4)_2$ superlattice grown at 400 °C (Castrucci *et al* 1998c). PL confirmed the structural results obtained by XAS and XPD and in particular detected Ge–Ge phonon vibrations only in the case of growth with surfactant action and growth at 400 °C (Pinto *et al* 1999).

2. Experimental details

X-ray absorption experiments were carried out at beamline SA 8 of the storage ring SuperACO (LURE, Orsay). A double-crystal monochromator with two beryl ($10\underline{1}0$) crystals allowed us to cover the photon energy range including the L edges of Ge with a resolving power better than 2000. All the measurements have been recorded in an ultra-high-vacuum chamber (base pressure $\sim 1 \times 10^{-10}$ mbar), in normal incidence (electric field parallel to the surface) in the Ge thin-film case, and at $\alpha = 45°$ incidence (i.e. the electric field vector forms an angle α with the surface normal) for Ge heterostructures. As an indirect measure of the absorption process, we recorded the total electron yield (TEY) emitted from the sample surface. Both the TEY and the incident photon flux I_0 were measured using a channeltron in pulse counting mode. All the spectra reported in this paper consist of the ratio between TEY and I_0 signals after a linear background subtraction. All the Ge/Si(001) samples were prepared *in situ* and characterized by low-energy electron diffraction (LEED). Silicon substrates were cleaned by Ar^+ sputtering and annealed up to 1100 °C until LEED showed a sharp double 2×1 pattern. Ge was evaporated from high-purity ingots by resistive heating of a tungsten basket. Evaporation rates and sample thicknesses were monitored by a quartz microbalance. For a few samples, Ge absolute coverages were determined *ex situ* by Rutherford back-scattering (RBS). By comparing XAS intensities of the reference and those measured for Ge/Si(001) samples, we obtained an evaluation ($\pm 15\%$) of the Ge deposited and a rough estimate of the depth probed by TEY in Ge case resulting to be around 100–150 Å. Different Ge monolayer coverages were deposited with the substrate kept at room temperature and subsequently annealed. Annealing procedures were performed at different temperatures, for 10 min each. All the samples analysed with XPD and the $(Ge_mSi_n)_p$ heterostructures were MBE (molecular beam epitaxy) grown at the Camerino University in a Riber SIVA 32 apparatus (base pressure $\leqslant 5.0 \times 10^{-11}$ Torr) equipped with three Knudsen cells for Ge, Si and Sb evaporation. Deposition rates were in the 0.3–1.0 Å min^{-1} range. Procedures to obtain good Si substrate reconstructions were described elsewhere (Gunnella *et al* 1996). Reflection high-energy electron diffraction (RHEED) and transmission electron microscopy (TEM) have been used to check sample quality and morphology, showing a highly oriented single crystal.

The Camerino University MBE apparatus is connected with an experimental chamber equipped with an x-ray aluminum Kα source and a Riber MacII electron analyser converted

to angular resolution by reducing the angular acceptance to ($6^\circ \times 6^\circ$) by screening 354° of the full circular aperture. A manipulator allowed the rotation of the sample in azimuthal and polar angle mode with an accuracy of 0.1° during XPD pattern acquisition.

PL measurements have been performed in a closed-circuit cryostat in the temperature range 10–300 K. We used an Ar^+ laser ($\lambda = 488$ nm) to excite the PL of the film. The laser power generally was about 100 mW cm^{-2}. For a few samples, i.e. the $(Ge_6Si_4)_p$, we used a power of 2 W cm^{-2}. The laser spot size was approximately 1 mm^2.

3. Ge/Si(001) interface and thin films

3.1. Growth without Sb action

For a long time, the first stages of Ge growth on Si(001) substrate have been extensively studied in terms of strain and surface morphology, thus neglecting any other possible mechanisms such as intermixing which can reduce the free energy of the system. Actually, total-energy calculations (Kelires 1994) and electron microscopy investigations (LeGoues *et al* 1990, Jesson *et al* 1991, 1992) have suggested the existence of a sizable degree of intermixing during the growth and/or subsequent annealing of Ge/Si heterostructures, but Ge segregation at only Si/Ge(001) interfaces has been generally accepted (Fukatsu *et al* 1991, Lin *et al* 1992). Despite the fact that several theoretical studies have suggested that a Ge–Si site exchange mechanism (Kelires and Tersoff 1989, Kelires 1994) is favoured due to the Si(001) surface 2×1 reconstruction, the behaviour of the Ge/Si(001) interface has been an open problem for several years. In fact, since only a few techniques are unambiguously able to distinguish intermixing from roughness and/or strain relief, very often intermixing at Ge/Si(001) interface has been reported not to occur. When we decided to investigate this interface only a few experiments were reported to observe the occurrence of intermixing at the Ge/Si(001) interface. Among them, surface extended x-ray absorption fine-structure measurements detected exchange mechanisms between Si and Ge after the second layer of Ge is deposited (Oyanagi *et al* 1994, 1995, Oyanagi 1992) and medium-energy ion scattering results suggested some degree of intermixing only after 3 ML of Ge deposition at 500 °C on the Si(001) substrate (Sasaki *et al* 1994). Nowadays several experiments agree that intermixing occurs both in the wetting layer (Voigtländer and Kästner 1999) and in the Ge islands, where it has been verified to be strongly dependent on the substrate temperature (Capellini *et al* 2001).

3.1.1. Ge critical coverage. As a first step, we studied the growth of 3 ML of Ge as a function of the temperature of the Si(001) substrate and of the subsequent annealings. The maximum value of the temperature was 450 °C. In figure 1 are reported the results of the Ge 3d XPD experiment from 3 ML Ge deposited at RT (middle curve) and at 400 °C (bottom curve). The measurements have been collected along the [110] direction and compared with the value of the anisotropy of the clean Si 2p XPD (top curve). Looking at figure 1, two main characteristics of the XPD patterns recorded for both temperatures used during the Ge deposition can be observed: (i) the presence of pronounced features in the diffraction patterns and (ii) the presence of an XPD peak in normal emission. The former point makes us easily conclude that Ge/Si(001), even at RT, grows in a crystalline way. In fact, with a sizeable disorder on the surface, these features would be replaced by a smooth background as observed on the 7×7-Si(111) surface (De Crescenzi *et al* 1995), where a large number of adsorption sites introduces a great degree of disorder and the growth of a polycrystalline layer occurs. Besides, the crystalline nature of the film is also confirmed by the undamped RHEED intensity oscillation measurements (Gunnella *et al* 1996). The presence of the XPD peak in normal

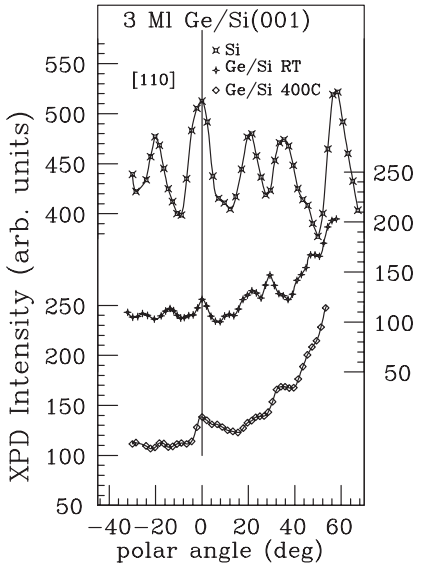

Figure 1. XPD from clean Si 2p of the 2 × 1-Si(001) surface (top curve) compared with the anisotropy of emission of Ge 3d electrons from 3 ML Ge deposition on the 2 × 1-Si(001) substrate taken at room temperature (middle curve) or with the substrate kept at 400 °C (bottom curve). The normal emission is emphasized by the vertical line.

emission is evidence of an increase, with respect to the nominal coverage, of the number of layers giving rise to the observed photoelectron diffraction signal. In fact, this peak can be originated only by electrons emitted by deep Ge atoms which are forward scattered by atoms located at least four planes below the surface. Actually, the presence of the 2 × 1 reconstruction destroys these paths, making necessary the existence of at least 6 ML thick Ge or Si/Ge overlayers. Similar results can be interpreted in terms of clusters and/or roughness formation on the surface (Diani *et al* 1993a, 1993b, Chambers and Loebs 1989) or as an hint of the occurrence of interdiffusion at the interface. However, the observation of well defined and elongated RHEED streaks leads us to exclude clusters and/or roughness formation (Gunnella *et al* 1996). We obtained similar conclusions by analysing the x-ray absorption data, namely:

(i) crystalline order even at RT deposition,
(ii) occurrence of intermixing. by analysing the x-ray absorption data.

Figure 2 reports the normalized experimental x-ray absorption at the Ge L_3 edge recorded for 3 ML Ge deposited at RT (solid circles) on the clean Si(001)-2 × 1 surface and after thermal annealing at 450 °C (open diamonds) (Castrucci *et al* 1998a). The two spectra show many similar features, though a general decrease in the intensity of the edge ($\leqslant 5\%$) and the presence of empty states at lower energies than that of the RT absorption edge can be observed after the annealing procedure. Similar changes in the XAS features have also been observed for samples annealed at 385 °C. Such small changes indicate the occurrence of some structural transformation during the annealing.

We had a closer look at the structural local order around Ge absorbing atoms by calculating the x-ray absorption profile for the most generally proposed growth model for 3 ML of Ge. The experimental spectrum of the RT Ge sample was not reproduced by the x-ray absorption spectra calculated by accounting for:

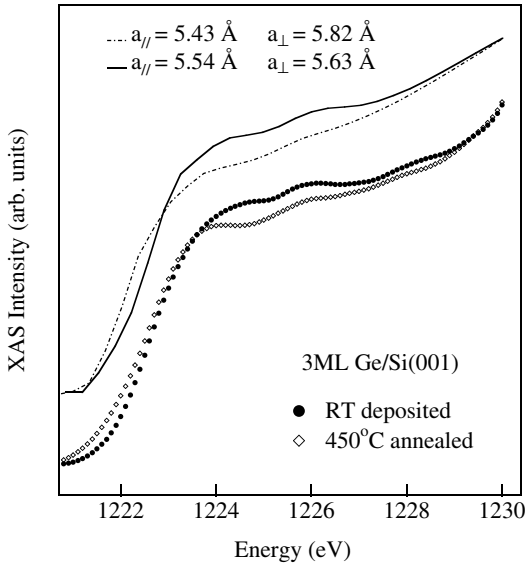

Figure 2. Experimental XAS features recorded for the as-deposited and annealed 3 ML Ge/Si(001) sample (solid circles and diamonds, respectively) compared with calculated x-ray absorption spectra for interface structural model b accounting for different values of strain. The solid curve relates to a fully strained overlayer, the dot–dashed curve to a partially relaxed one. Both experimental and theoretical curves have been smoothed and normalized to the same arbitrary value far from the absorption edge.

(i) a Ge layer-by-layer growth,
(ii) several heights and distribution of Ge terraces to give roughness,
(iii) a Ge intermixing accounting for the formation of a zincblende alloy, illustrated in figure 3 left panel (a) and
(iv) an interface rearrangement where the atoms reaccommodate as drawn in figure 3 left panel (c).

On the contrary, a model which took into account a Ge–Si atom exchange mechanism sketched in figure 3 left panel (b) has been found to best mimic the experimental data (see figure 3, right panel). Since both roughness and intermixing have been considered to occur in order to reduce the total energy of the system, in all the reported calculations no strain relief has been accounted for, so Ge fully strained lattice parameters have been used ($a_{\mathrm{Ge}\perp} = 5.82$ Å). Moreover, the reconstruction of the top Ge layer has been introduced by a simple symmetric dimer model (Oyanagi *et al* 1994, 1995, Oyanagi 1992). In figure 2 (top panel) we also reported the best simulation of the x-ray absorption spectrum (continuous curve) that we obtained for the RT-deposited sample and we compared it with a calculation performed by using the same intermixing growth model but partially relaxed (dot–dashed curve). This latter spectrum has been obtained by introducing in-plane and out-of-plane lattice parameters of 5.54 and 5.63 Å respectively. Interestingly, experimental XAS measured on the annealed samples (open diamonds, lower panel) more closely resembles the dot–dashed curve. In particular, the increase of empty states around the absorption edge energies after the annealing is well reproduced by XAS calculations on a partially relaxed system. The same physical effect has been also observed in RHEED experiments (Miki *et al* 1989, Gunnella *et al* 1996, Showalter *et al* 1996).

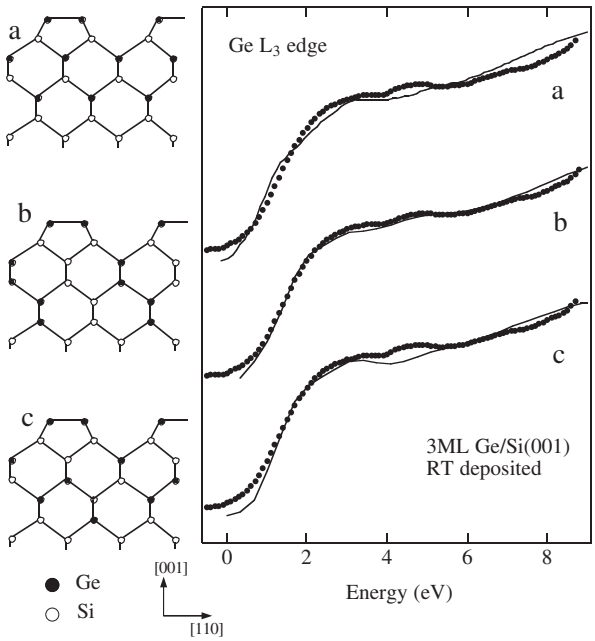

Figure 3. Left panel: different structural models of the Ge/Si(001) interface projected along [001] and [110] axes. Right panel: comparison between experimental features recorded for RT-deposited 3 ML Ge/Si(001) interface and calculated x-ray absorption spectra obtained introducing models a–c.

3.1.2. Ge coverages above the critical thickness. Several samples have been investigated with a Ge thickness above the critical one. Among these, the ones that we considered most interesting are those grown by nominally depositing 6 ML of Ge. Their RHEED patterns evidenced the appearance of spots (which indicate a transition to a three-dimensional growth) and of an expansion by 2% of the in-plane lattice parameter occurring between 2.4 and 3.6 ML (Gunnella *et al* 1996), thus involving only the outermost Ge layers. In figure 4 we report the experimental XPD patterns (crosses) recorded for Ge deposition at 400 °C on the Si(001) surface. The best fits between experiment and theory (figure 4, solid curves), for both the azimuthal directions, have been obtained by considering five layers of Ge atoms plus a sixth one, introduced to account for the surface reconstruction, a tetragonal distorted out-of-plane lattice parameter of 5.75 ± 0.02 Å pseudomorphic on the Si in-plane lattice parameter. The reconstruction has been introduced by a simple symmetric dimer model of the Ge top layer (Oyanagi *et al* 1994, 1995, Oyanagi 1992). The same results of the fitting procedure have been obtained for AED patterns (figure 5, bottom) reported by Diani and co-workers 1993a for a similar sample grown under the same experimental conditions on a vicinal silicon surface cut at 4° to the [110] direction. Moreover, it has been reported in the literature that the XPD anisotropy, during Ge island formation on a wetting layer of 3–4 ML, does not substantially change with respect to that given by the thermodynamically stable continuous wetting layer (Diani *et al* 1993a). On the other hand, from a careful analysis of the width of the diffraction features (figure 4) along the [101] direction, it is possible to conclude that our experimental XPD signal is basically built up by six strained Ge atomic layers. In fact, any other contribution induced by unstrained Ge islands or roughness would produce a broadening and a possible shift toward the value relating to an unstrained film; furthermore, no reproduction of the correct

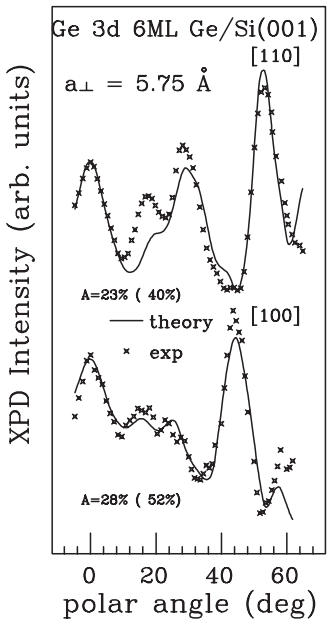

Figure 4. Best-fit comparison between theory and experiment for the case of XPD of the Ge 3d core level from 6 ML of Ge deposited on the 2×1-Si(001) substrate kept at 400 °C. The emission direction is along [110] (top curves) and along [100] (bottom curves). A value of 5.75 ± 0.02 Å for the out-of-plane lattice parameter in the Ge overlayer is obtained. The value of the in-plane lattice parameter is 5.43 Å. Values of the XPD anisotropy for the experimental and theoretical curves are reported.

anisotropy can be obtained. From this analysis we conclude that the contribution of the Ge islands is negligible and that the six planes we need to fit the experimental data are due to the existence of an intermixed phase. As a matter of fact, this means that:

(a) our experimental XPD patterns are mostly sensitive to the wetting layer,
(b) no hints of roughness can be detected for the wetting layer and
(c) the presence of intermixing can be invoked (Gunnella *et al* 1996).

Finally, we interpret our experimental results as due to the following growth process: in the presence of a sufficiently high temperature of the substrate, evaporation of dimer rows is possible for Ge thickness lower than 3 ML (Köhler *et al* 1992, Horn von Hoegen *et al* 1994), resulting in a partial relaxation of the strain ($a_{\mathrm{Ge}\perp} = 5.75 \pm 0.02$ Å); as the in-plane lattice parameter keeps on relaxing, as we observed by RHEED, growth of coherent islands on a partially strained film occurs with a substantial relaxation of the strain energy. During the growth Ge–Si exchange mechanisms occur (Gunnella *et al* 1996). The same analyses have been applied to AED curves reported by Diani and co-workers 1993a for 6 ML of Ge, deposited at RT, on a vicinal Si(001) surface cut at 4° to the [110] direction. The best fit (figure 5, top, solid curves) of the RT experiment (figure 5 top, dot–dashed curve) has been obtained with nine planes of scatterers and an $a_{\mathrm{Ge}\perp}$ value of 5.82 ± 0.02 Å. This means that to build up all the features needed to reproduce the XPD patterns a larger number of layers than a nominal thickness is necessary. These results suggest that an important interdiffusion process occurs even at room temperature. Moreover, in this case, the lack of strain relaxation (dimer row evaporation) or roughness well explains the higher value of the tetragonal distortion

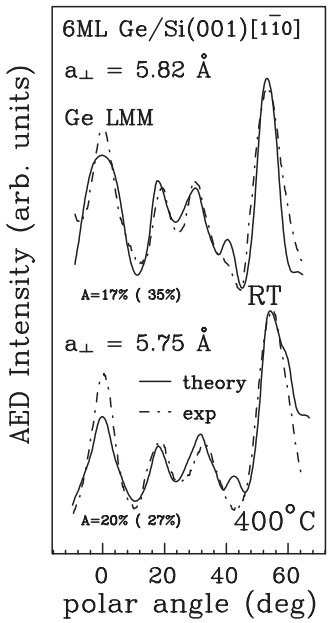

Figure 5. Best fit of an experiment performed by Diani and collaborators at the Ge LMM (1146 eV) Auger level on a vicinal surface cut at 4° to the [110] direction. Polar patterns are taken along the [1$\bar{1}$0] direction. The top experimental curve relates to deposition of 6 ML of Ge at RT while the bottom one is 6 ML deposition on the sample kept at 400 °C. In the RT case nine planes of Ge were necessary to fit experimental data. A value of 5.82 ± 0.02 Å for the out-of-plane lattice parameter is obtained, while a value of 5.75 ± 0.02 Å was found for the 400 °C experiment. The values of the AED anisotropy for the experimental and theoretical curves are reported.

of 5.82 ± 0.02 Å obtained. This value is in good agreement with the value provided by the elasticity theory and turned out to be higher than the value found for the deposition at 400 °C (Gunnella *et al* 1996).

3.2. Sb-modified growth

During Sb-assisted growth deposition, the clean Si(001) surface was kept at a temperature ranging between 500 and 700 °C, while a partial pressure of Sb of the order of 10^{-7} mbar from the Sb Knudsen cell was directed towards the sample. A short annealing at 600 °C was used to get rid of Sb in excess of about 1 ML on the 2×1-Sb/Si(001) surface observed by RHEED.

XPS profiles confirmed the presence of about 1 ML of Sb when compared with the photoemission signal from Ge. Typically the value reported in the literature for the deposition is between 0.7 and 0.8 ML (Slijkerman *et al* 1992). In figure 6 are reported the XPD measurements obtained for Si 2p and Sb 3d along the [001] direction after deposition of 1 ML of Sb on the clean Si(001) substrate. In this figure the Si 2p diffraction pattern shows the characteristic fingerprints of the diamond cubic structure while the diffraction pattern obtained from the Sb 3d core level shows only a smooth instrumental background. This shows the lack of incorporation of Sb atoms into the Si matrix. The same behaviour of Sb 3d core-level patterns has been also measured with successive deposition of Ge layers, showing evidence of floating to the surface of the whole Sb layer.

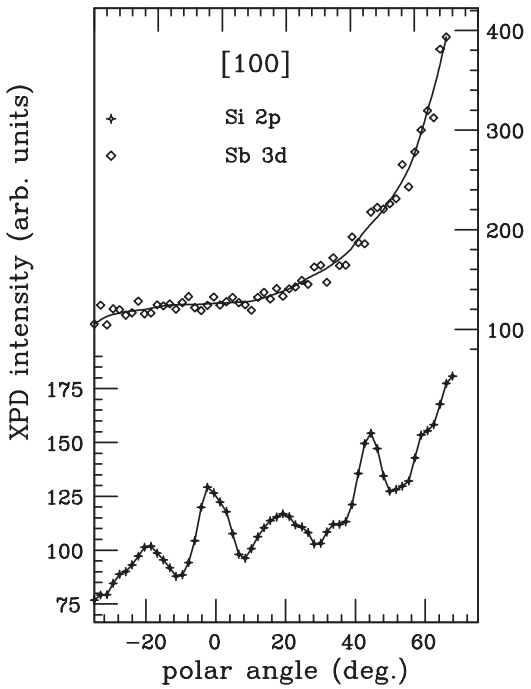

Figure 6. XPD of 1 ML Sb/Si(001). The top curve represents the instrumental response of the apparatus only; in fact, no diffraction features can be observed on the polar diagram of Sb 3d. In the lower curve is reported the pattern of Si 2p. The direction of emission is [100].

3.2.1. Ge critical thickness. In figure 7 are reported the polar patterns of the Ge LMM Auger level along the [100] direction for 3 ML of Ge grown at 400 °C on the 2 × 1-1 ML Sb/Si(001) surface (curve (a)) and for the successive deposition of 3 ML of Si at 400 °C as a cap layer (curve (c)). Curve (b) reports the Si 2p XPD polar pattern of the reference. The normalized multiple-scattering calculations are reported on the experimental points as full lines. In the simulation a double-domain 2 × 1 reconstructed surface with Sb termination is considered, as checked by RHEED. In curve (a) of figure 7 there can be detected a few diffraction peaks, but none close to normal emission (0°), which represents the fingerprint of scattering of a total of five planes in the diamond unit. This indicates that the overlayer has a full crystal structure but that no interdiffusion or roughness takes place at this stage of the Ge growth. In addition, from the analysis of the angular shift of the characteristic peaks at 45° along [100], compared with the unshifted Si 2p peak, the amount of strain in the film, and the relative value of the out-of-plane lattice parameter, have been evaluated. Such a determination has been carried out by comparison with multiple-scattering calculations. Considering the reconstructed top layer of Sb atoms, the calculations have shown the best agreement with the 3 ML of epitaxial Ge grown with a value of the out-of-plane lattice parameter of 5.78 ± 0.06 Å. We stress that in this case the lower value of the anisotropy increases the error bar on this determination. In any case, the value of the out-of-plane lattice parameter found is close to the value of the tetragonal distortion evaluated by the classical theory of elasticity.

Curve (c) of figure 7 shows the AED polar patterns of Ge LMM for 3 ML of Ge epitaxially grown on Si(001) and a subsequent deposition of a cap layer of 3 ML of Si. As can be appreciated by visual inspection, a minor shift of the diffraction features is obtained in this

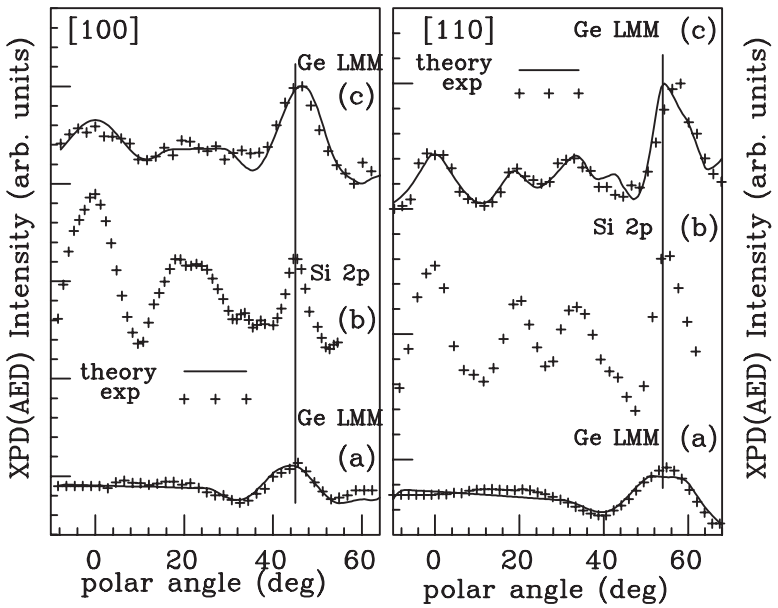

Figure 7. AED polar pattern along the [100] direction: (a) Ge LMM Auger polar pattern of 3 ML Ge/1 ML Sb/Si(001) grown at 400 °C; (b) Si 2p XPD; (c) Ge LMM of 3 ML Si/3 ML Ge/1 ML Sb/Si(001) grown at 400 °C. On curves (a) and (c) are reported the normalized multiple-scattering calculations which best fit the experiment. The 3 ML of Ge are tetragonally distorted. The obtained value of the out-of-plane lattice parameter is equal to 5.78 ± 0.06 Å, curve (a), and 5.82 ± 0.02 Å, curve (c).

case, but the value of the out-of-plane lattice parameter in the calculated patterns turned out to be the same as that determined for curve (a). In this case, in fact, the effect of the angular shift is obscured by the epitaxially grown unstrained Si layers, which reduce the angular shift sensitivity to the value of the Ge film tetragonal distortion. Besides, due to the high sensitivity of the XPD technique to the number of emitter planes, the curve (c) best fit is found to occur only in the case of a sharp interface between the epitaxially grown overlayers, thus showing no segregation of Ge into the Si cap layer. This lack of any intermixing effects confirmed the assumption that the strain is fully maintained even after the deposition of a Si cap layer. This enforces the relationship between atomic exchange effects and strain induced by the reconstruction, which turns out to be considerably reduced in the presence of Sb as a surfactant. In figure 8 are reported the polar patterns of the Ge LMM Auger level for 3 ML of Ge deposited on a Sb/Si(001) surface. The measurements performed after deposition at RT are compared with those taken after the annealing of the sample at 600 °C for 15 min. In this case, the AED is able to show that even at RT the Ge grows in a crystalline form because of the characteristic features of AED patterns for this nominal thickness. Furthermore no effects induced by intermixing and/or roughness can be detected as no normal emission peaks are present along the [100] and [110] directions. After the annealing at 600 °C the appearance of the intensity peak at 0° polar angle emission is a fingerprint contribution to AED of five or six layers, thus indicating that, in principle, some roughness and/or intermixing of Ge atoms into Si matrix has occurred.

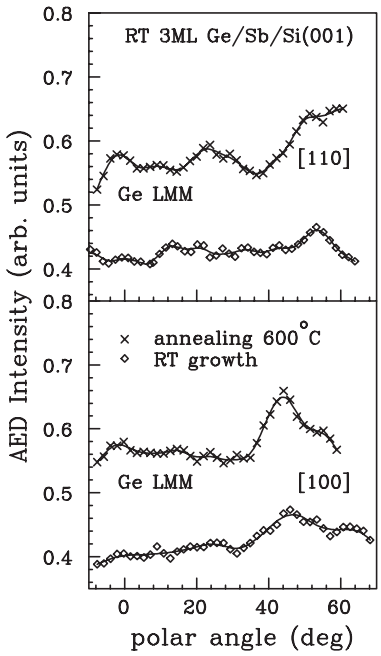

Figure 8. Polar AED measurements along [110] (top) and [100] (bottom) directions of Ge LMM after 3 ML of Ge deposition on 1 ML Sb/Si(001) substrate kept at RT and subsequently annealed at 600 °C.

3.2.2. Ge coverages above the critical thickness. In the case of 6 ML deposition of Ge on the 2×1-1 ML Sb/Si(001) surface, we kept the sample at 400 °C during evaporation. In figure 9 is reported the best fit for 6 ML of Sb-mediated growth of Ge (solid curve) and the experimental AED patterns (crosses). As can be observed, a great amount of strain (corresponding to a perpendicular lattice parameter $a_\perp = 5.82 \pm 0.02$ Å) is obtained after the fit. This value of the out-of-plane lattice parameter is in fair agreement with its determination in the case of 3 ML of Ge grown in the same conditions, while differences with the Ge/Si(001) samples grown at 400 °C without surfactants are sizeable and well exceed the error in the angle determination. In addition, the RHEED pattern, monitored during the growth, also gave no hints of relaxation of the in-plane lattice parameter or of island formation during the growth with Sb.

4. $(Ge_nSi_n)_p$/Si(001) heterostructures

In the case of $(Ge_nSi_n)_p$ heterostructures we explored the possibility of growing superlattices directly on the Si(001) substrate kept at 400 °C. In figure 10 we report the experimental Ge L_3 x-ray absorption near-edge spectra (triangles and diamonds) recorded for two heterostructures, $(Ge_2Si_2)_{15}$/Si(001) and $(Ge_4Si_4)_2$/Sb/Si(001), compared with the corresponding calculated spectra for the two nominal heterostructures (solid curves). This means that each interface has been considered atomically sharp and strained to the substrate lattice. While the energy positions of the observed experimental features and their relative intensities have been rather well reproduced by calculation, no accordance is found between the measured and the simulated spectra reported in the upper part of figure 10 for the $(Ge_2Si_2)_{15}$/Si(001) heterostructure. These results are consistent with our studies on the Ge/Si(001) ultra-thin films presented in the

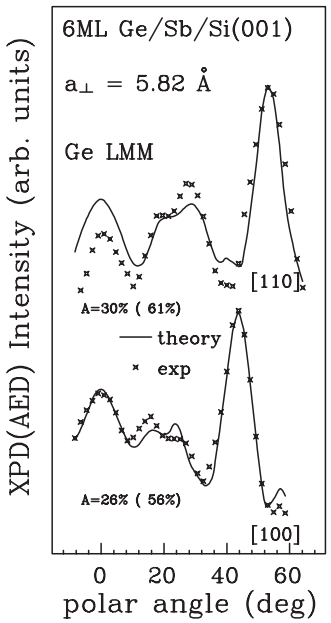

Figure 9. Best-fit comparison between theory and experiment for the case of XPD of the Ge Auger LMM level from 6 ML of Ge deposited on the 1 ML Sb-2 × 1-Si(001) substrate kept at 400 °C. The emission direction is along [110] (top curves) and along [100] (bottom curves). A value of 5.82 ± 0.02 Å for the out-of-plane lattice parameter in the Ge overlayer was found. The values of the AED anisotropy for the experimental and theoretical curves are reported.

sections above, where the intermixing process at the silicon interface has been detected for those Ge films prepared without surfactant. Similarly, in the literature Ge has been observed to segregate to the silicon layers deposited above (LeGoues *et al* 1989, Yang *et al* 1992). Since the $(Ge_2Si_2)_{15}$ system is characterized by a very small thickness of nominally pure element layers, we assumed that the exchange phenomenon is likely to involve almost completely each period, giving rise approximately to a $Ge_{0.5}Si_{0.5}$ alloy phase. In figure 12 we report the calculations of the x-ray absorption spectra for three different alloy models. The dashed and dot–dashed curves have been calculated for the two rhombohedral structures (RSs), the so-called RS1 and RS2 alloy models shown in figure 12. The dotted curve has been obtained for a SiGe zincblende structure. By comparing the theoretical spectra and the experiment (figure 11, black circles) a good accordance can be found for the RS1 model. This alloy model has been considered to be the most favourable because it is microscopically unstrained. The coexistence of RS1 and RS2 structural configurations appears unlikely, according to the relative intensities of four main features constituting the Ge L_3 absorption edge. This coexistence would smear out the B and D structures, peculiar to the RS1 model, and conversely would enhance the A feature, in strong disagreement with the experimental intensities. In any case, the ensemble of the proposed models is not the exhaustive one, especially if we admit that the ordering mechanism of the alloy might not occur along well defined crystallographic directions (Aebi *et al* 1992). In particular we are not able to treat the cases in which Ge- or Si-rich sites have to be accounted for with a well defined ratio (different from zero or unity) of the atomic population (e.g. RS3 alloy models) (Jesson *et al* 1993). In fact the choice of the models has been driven by the need for a high degree of symmetry necessary to reduce the number of configurations to account for in the *ab initio* calculations. Finally, these results are not in

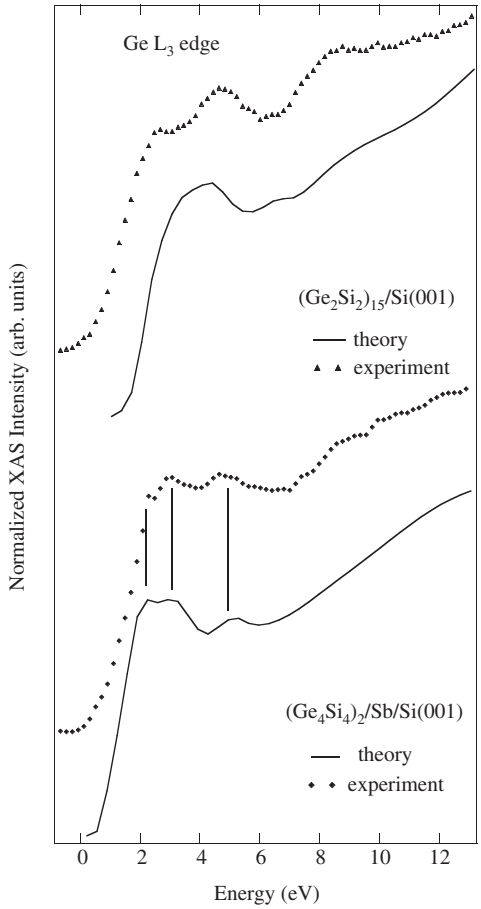

Figure 10. Comparison between the experimental Ge L_3 x-ray absorption spectra of the $(Ge_2Si_2)_{15}$ multilayer grown on the Si(001) substrate (triangles) and a theoretical curve calculated for the corresponding strained superlattice structure. Comparison between the experimental Ge L_3 x-ray absorption spectra of the $(Ge_4Si_4)_2$ multilayer deposited on the Sb/Si(001) substrate (diamonds) and a theoretical curve calculated for the corresponding strained heterostructure.

contrast to the interdiffusion model that we obtained for the 3 ML Ge/Si(001) interface. In fact, the two systems are intrinsically different: in one case the thin film mostly experiences non-equilibrium conditions and the intermixing mechanism is due to the strains induced by the silicon surface 2×1 reconstruction; in the other case the $(Ge_2Si_2)_{15}$ system can reach the more stable ordered alloy phase (RS1) by the additional process of segregation at Ge/Si interface.

5. Photoluminescence

Several samples have been investigated by performing PL experiments. The main goal was to study the evolution of the PL emission by changing the growth conditions, temperature and surfactant effect. In fact, PL measurements allow one to study the bandgap and the presence of radiative channels. Information about morphological properties (islanding and

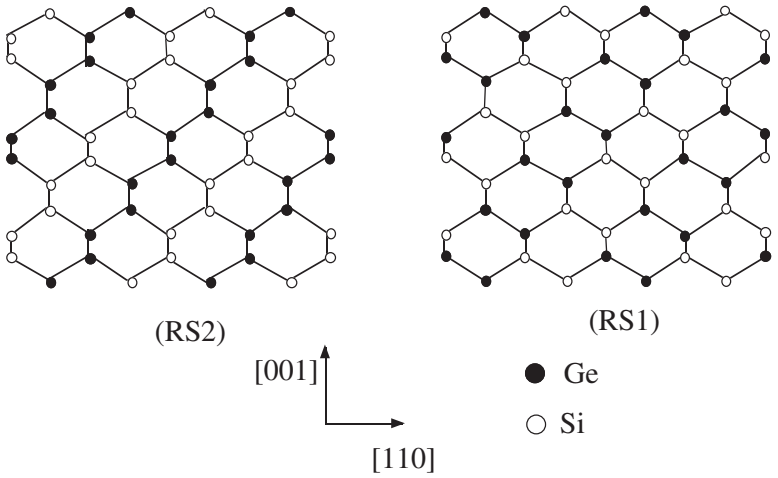

Figure 11. Stick and ball sketches of two among the Ge–Si alloy models proposed in the literature: in the structures reported each atom is characterized by three (RS1, right panel) and one (RS2, left panel) heteropolar bonds.

defects) and alloy formation can be also obtained (Vescan *et al* 1992, Menczigar *et al* 1992, Souifi *et al* 1995, Loo *et al* 2001). We recorded the PL spectrum for $Ge_{0.2}Si_{0.8}$/Si(001) and $Ge_{0.5}Si_{0.5}$/Si(001) alloys both grown at 400 °C, capped with a 3 nm silicon film and 3 and 10 nm thick respectively (figures 13(a) and (b)). We compared these spectra with that of a Si substrate that does not show any features in the range 0.8–1.0 eV and is dominated by the transverse optical (TO) peak located at 1.1 eV. We observed that by decreasing the Ge concentration in the alloy the PL peaks shifted towards the silicon feature. In figure 13(b) are recognized the no-phonon (NP) peak and the series of phonons located at lower energies while in figure 13(a) the NP feature superimposes on the silicon TO line. In particular the energy difference between the $TO_{Si–Si}$ and the NP features turned out to be about 60 meV, while the TA (transverse-acoustical phonon), $TO_{Si–Ge}$ and $TO_{Ge–Ge}$ appear between these two features. The sharpness of the different features observed in the spectra has been shown to be sensitive to thickness and/or composition fluctuations (Vescan *et al* 1992). In figure 13(c) is also reported the PL spectrum of a sample constituted by 12 nm of Ge deposited at 600 °C on a Sb/Si(001) substrate. We note that the PL spectrum resembles that of $Ge_{0.5}Si_{0.5}$/Si(001) alloy, but shows a further broad feature located about 0.8 eV that can be ascribed to island formation (Loo *et al* 2001). A sample prepared by depositing 6 ML of Ge on a Sb/Si(001) surface kept at 500 °C also appeared to show a similar PL behaviour, thus indicating that in this case the surfactant action is reduced both in islanding and intermixing prevention (figure 13(d)). During the last decade the PL features have been detected and/or improved for MBE-grown samples only after a thermal treatment at high temperature ($T = 600$–900 °C) (Brunner *et al* 1992) or after an annealing in H_2 atmosphere at low temperature (400–450 °C) (Dettmer and Weber 1992, Bremond *et al* 1992). In our case the PL features are present after deposition at low temperature (400–450 °C) and this observation deserves further studies to understand more deeply the role of temperature and the growth conditions to fully control the formation of misfit dislocation and defects. Figure 14 shows the normalized PL spectra recorded for $(Ge_4Si_6)_p$ ($p = 1, 2, 10, 30$) strained-layer superlattices grown in the presence of Sb with the silicon substrate kept at 400 °C. Two main lines located at 1.02 eV (TO) and 1.06 eV (NP) can be observed in the PL spectra which are insensitive to the heterostructure repetition number.

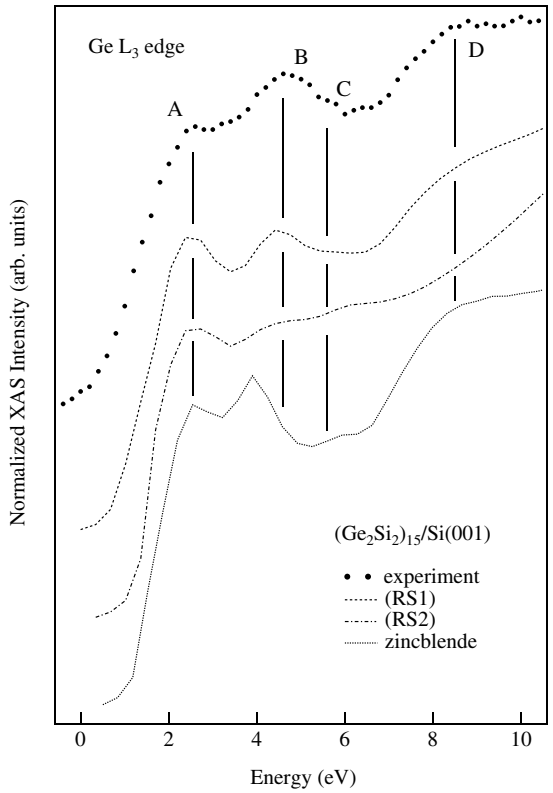

Figure 12. Comparison between the experimental Ge L_3 x-ray absorption spectra of the $(Ge_2Si_2)_{15}$ multilayer grown on the Si(001) substrate (black circles) and theoretical curves calculated for several $Ge_{0.5}Si_{0.5}$ alloy models fully strained to the substrate: RS1 (dashed curve), RS2 (dot–dashed curve) and zincblende (dotted curve).

No other features below 0.95 eV were detected in the spectra, confirming the absence of alloy formation induced by the intermixing at the interface. The energy difference between the TO and NP features amounts to about 40 meV, which is in good agreement with a value reported by (De Gironcoli 1992) for TO phonons of Ge–Ge vibrations. The reported considerations suggested that the PL processes cannot be generated by the superperiodicity of the extended superlattices, but it should be attributed to a local process involving excitonic recombination occurring mainly in the Ge layers. Within this picture, the excitonic wavefunction is sufficiently localized to involve few Ge–Ge pairs whatever the overgrown structure is, explaining the reason why the repetition number does not affect the energy position, intensities or broadening of the single-quantum-well features. This PL measurement confirmed that to grow superlattices and Ge films by keeping the substrate at temperatures higher than 500 °C strongly reduced the surfactant action, therefore leading to the formation of an intermixed wetting layer at the interface and islanding. Thus, in our opinion, the only way to obtain a tunable direct or quasi-direct gap due to the zone-folding effect is to grow the Ge-based samples at low temperature (about 400 °C) and with the aid of surfactants.

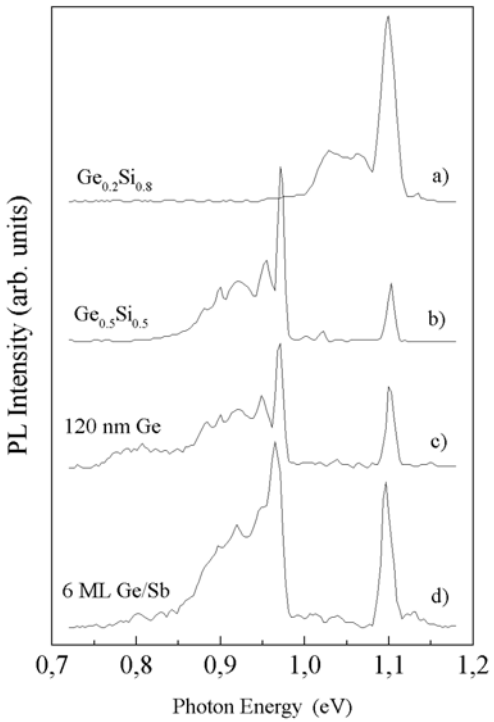

Figure 13. PL spectra at $T = 10$ K of (a) $Ge_{0.2}Si_{0.8}$ alloy grown on Si(001), (b) $Ge_{0.5}Si_{0.5}$ alloy grown on Si(001), (c) 12 nm of Ge grown on Sb/Si(001) and (d) 6 nm of Ge grown on Sb/Si(001) excited with $P = 100$ mW cm^{-2} laser radiation of 488 nm from an Ar^+ laser.

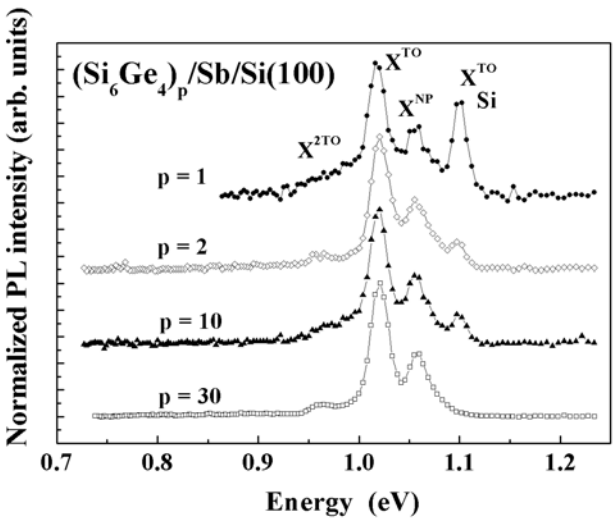

Figure 14. PL spectra at $T = 10$ K of $(Ge_4Si_6)_p$ superlattice grown on Si(001) excited with a $P = 2$ W cm^{-2} laser radiation of 488 nm from an Ar^+ laser.

6. Conclusions

Evaluation of the interface quality is a very important task in heteroepitaxial growth. An experimental probe able to provide information on the quality level of interfaces in terms of intermixing, roughness, three-dimensional island formation and quantification of strain relaxation is a precious tool. In this report we have reviewed our recent works on the interdiffusion process, roughness formation and strain relief mechanisms occurring at the first stages of Ge growth and for GeSi heterostructures with and without the surfactant action by XAS and XPD. The growth or the annealing temperature even in the presence of Sb has been found to be crucial to obtain sharp Ge/Si interfaces. Also PL spectra gave us information on interdiffusion and islanding. In particular, we observed phonon vibrations typical of Ge–Ge pairs in the case of $(Ge_4Si_6)_p$ superlattices grown in the presence of Sb and at 400 °C.

References

Aebi P, Tyliszczak T, Hitchcock A P, Baines K M, Sham T K, Jackman T E, Baribeau J M and Lockwood D J 1992 *Phys. Rev.* B **45** 13 579

Bremond G, Souifi A, Benyattou T and Dutartre D 1992 *Thin Solid Films* **222** 60

Brunner J, Menczigar U, Gail M, Friess E and Abstreiter G 1992 *Thin Solid Films* **222** 27

Capellini G, De Seta M and Evangelisti F 2001 *Appl. Phys. Lett.* **78** 303

Castrucci P, Gunnella R, De Crescenzi M, Sacchi M, Dufour G and Rochet F 1998a *Phys. Rev.* B **58** 4095

Castrucci P, Gunnella R, De Crescenzi M, Sacchi M, Dufour G and Rochet F 1998b *J. Vac. Sci. Technol.* B **16** 1616

Castrucci P, Gunnella R, Pinto N, De Crescenzi M, Sacchi M, Dufour G and Rochet F 1998c *Surf. Sci.* **416** 466

Chambers S A and Loebs V A 1989 *Phys. Rev. Lett.* **63** 640

Chambers S A and Loebs V A 1990 *Phys. Rev.* B **42** 5109

Copel M, Reuter M C, Kaxiras E and Tromp R M 1989 *Phys. Rev. Lett.* **63** 632

Copel M and Tromp R M 1991 *Appl. Phys. Lett.* **58** 2648

De Crescenzi M, Gunnella R, Bernardini R, De Marco M and Davoli I 1995 *Phys. Rev.* B **52** 1806

De Gironcoli S 1992 *Phys. Rev.* B **46** 2412

Dettmer K and Weber J 1992 *Thin Solid Films* **222** 234

Diani M, Bishoff J L, Kubler L and Bolmont D 1993a *J. Appl. Phys.* **73** 5621

Diani M, Aubel D, Bishoff J L, Kubler L and Bolmont D 1993b *Surf. Sci.* **291** 110 and references therein

Egelhoff W F Jr 1990 *Crit. Rev. Solid State Mater. Sci.* **16** 213

Fadley C S 1990 *Synchrotron Radiation Research: Advances in Surface Science* ed Z Bachrach (New York: Plenum) and references therein

Fukatsu S, Fujita K, Yaguchi H, Shiraki H and Ito R 1991 *Appl. Phys. Lett.* **59** 2130

Gunnella R, Castrucci P, Pinto N, Davoli I, Sebilleau D and De Crescenzi M 1996 *Phys. Rev.* B **54** 8882

Gunnella R, Castrucci P, Pinto N, Cucculelli P, Davoli I, Sebilleau D and De Crescenzi M 1998 *Surf. Rev. Lett.* **5** 157–61

Horn von Hoegen M, Müller B H and Al-Falou A 1994 *Phys. Rev.* B **50** 11 640

Jesson J D, Pennycock S J and Baribeau J M 1991 *Phys. Rev. Lett.* **66** 750

Jesson D E, Pennycock S J, Baribeau J M and Houghton D C 1992 *Phys. Rev. Lett.* **68** 2062

Jesson D E, Pennycock S J, Tishler J Z, Budai J D, Baribeau J M and Houghton D C 1993 *Phys. Rev. Lett.* **70** 2293

Kelires P C and Tersoff J 1989 *Phys. Rev. Lett.* **63** 1164

Kelires P C 1994 *Phys. Rev.* B **49** 11 496

Köhler U, Jusko O, Müller B H, Horn von Hoegen M and Pook M 1992 *Ultramicroscopy* **42–4** 832

LeGoues F K, Copel M and Tromp R M 1989 *Phys. Rev. Lett.* **63** 1826

LeGoues F K, Kesan V P, Iyer S S, Tersoff J and Tromp R 1990 *Phys. Rev. Lett.* **64** 2038

Lin D S, Miller T and Chiang T C 1992 *Phys. Rev.* B **45** 11 415

Loo R, Meunier-Beillard P, Vanhaeren D, Bender H, Caymax M, Vandervorst W, Dentel D, Goryll M and Vescan L 2001 *J. Appl. Phys.* **90** 2565

Menczigar U, Brunner J, Friess E, Gail M, Abstreiter G, Kibbel H, Presting H and Kasper E 1992 *Thin Solid Films* **222** 227 and references therein

Miki K, Sakamoto H and Sakamoto T 1989 *Chemistry and Defects in Semiconductor Heterostructures (MRS Symp. Proc. No 148)* ed M Kawabe, T O Sands, E R Weber and R S Williams (Pittsburgh, PA: Materials Research Society) p 323

Noel J P, Greene J E, Rowell N L, Kechang S and Houghton D C 1989 *Appl. Phys. Lett.* **55** 1525
Noel J P, Greene J E, Rowell N L and Houghton D C 1990 *Appl. Phys. Lett.* **56** 265
Oyanagi H 1992 *Appl. Surf. Sci.* **60/61** 522
Oyanagi H, Sakamoto K, Shioda R and Sakamoto T 1994 *Japan. J. Appl. Phys.* **33** 3545
Oyanagi H, Sakamoto K, Shioda R, Kuwahara Y and Haga K 1995 *Phys. Rev.* B **52** 5824
Pearsall T P, Vanderberg J M, Hull R and Bonar J M 1989 *Phys. Rev. Lett.* **63** 2104
Pinto N, Tombolini F, Murri R, De Crescenzi M, Casalboni M, Barucca G and Majni G 1999 *Surf. Sci.* **437** 145
Presting H, Kibbel H, Jaros M, Turton R M, Menczigar U, Abstreiter G and Grimmeiss H G 1992 *Semicond. Sci. Technol.* **7** 1127
Sasaki M, Abukawa T, Yeom H W, Yamada M, Suzuki S, Sato S and Kono S 1994 *Appl. Surf. Sci.* **82/83** 387
Schmid U, Christensen N E, Alouani M and Cardona M 1991 *Phys. Rev.* B **43** 14 597
Showalter J H, Deelman P W and Thundat T 1996 *Appl. Surf. Sci.* **104/105** 510
Slijkerman W F J, Zagwijn P M, van der Veen J F, Garvesteijn D J and van de Walle J F A 1992 *Surf. Sci.* **262** 25
Souifi A, Benyattou T, Guillot G, Bremond G, Dutartre D and Warren P 1995 *J. Appl. Phys.* **78** 4039
Stöhr J 1992 *NEXAFS Spectroscopy (Springer Series in Surface Science vol 25)* ed R Gomer (Berlin: Springer)
Tserbak C, Polatoglou H M and Theodoru G 1993 *Phys. Rev.* B **47** 7104
Vescan L, Schmidt K, Dieker C, Tang H P, Vescan T and Lüth H 1992 *Thin Solid Films* **222** 5
Voigtländer B and Kästner M 1999 *Phys. Rev.* B **60** R5121
Yang X, Cao R, Terry J and Pianetta P 1992 *J. Vac. Sci. Technol.* B **10** 2013
Zachai R, Eberl K, Abstreiter G, Kasper E and Kibbel H 1990 *Phys. Rev. Lett.* **64** 1055